

Unusually Strong Temperature Dependence of Graphene Electron Mobility

Akin Akturk and Neil Goldsman

Department of Electrical and Computer Engineering,
University of Maryland, College Park, MD, USA
akturka@umd.edu

Abstract—We report unusually strong temperature dependence of graphene electron mobility, obtained using full-band Monte Carlo (MC) simulations and experiment. The electron-phonon scattering limited intrinsic graphene electron mobility changes by as much as the fourth power of temperature, T^n ($2 < n < 4$), in the 200 K to 350 K range. This is in contradiction with the generally observed approximately linear T dependence around room temperature. This linear dependence arises due to the phonon equipartition approximation that gives rise to a linear temperature versus scattering rate relation. The highly nonlinear temperature dependence is reminiscent of transport in the Bloch-Grüneisen temperature range, where phonon energies assisting emissions and absorptions are less than or comparable to thermal energies. In addition, graphene has a conic dispersion relation around its K points or conduction band minima, setting it apart from other materials with parabolic energy-momentum curves around their conduction band minima, and consequently well-defined effective masses.

Keywords—graphene mobility; temperature dependence; Bloch-Grüneisen temperature dependence; graphene mobility temperature dependence.

I. INTRODUCTION

Graphene has recently created an excitement among researchers due its very high measured and calculated low-field mobility values [1-5], approaching $1\text{-}2 \times 10^5$ cm^2/Vs . This mobility limit is significantly larger, as much as hundred times compared to the silicon's, than the room temperature low-field mobilities associated with semiconductor materials. In addition to having very high intrinsic low-field mobilities, it exhibits an unconventional quantum Hall effect and a minimum conductivity [1-4]. Also, its electrons at or near conduction band minima do not have well-defined effective masses due to the conic shape of its dispersion curve in the vicinity of these points, as shown in Fig. 1. This may cause them act as Dirac fermions with kinetic energies $m_0 v^2$ where m_0 is the free electron mass and v is the graphene electron Fermi velocity, which is one three-hundredth of the speed of light.

Graphene is a two-dimensional single planar layer of graphite sheet, and is the building block of one-dimensional carbon nanotubes and nanoribbons, and zero-dimensional fullerenes. As the mechanical exfoliation method or the so-called "Scotch-tape method" has recently enabled quick and less strenuous preparation of graphene, a rise in the number of measurements and theoretical work to obtain its electrical

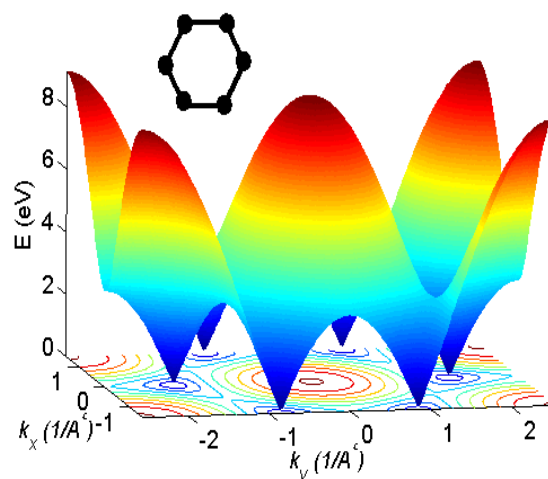


Figure 1. Energy dispersion curve of graphene with an hexagon shaped unit cell shown above. Conduction band touches the valence band at the six K points as shown above, making graphene a semi-metal.

characterization has followed. However, the earlier experimental analyses have proven it to be hard to extract graphene properties, as being a very thin layer, graphene has interacted strongly with its environment via remote scatterers. Also, local impurities on graphene samples have overwhelmed measurements as acting near scatterers [6]. However, these are extrinsic factors, and are not representative of the material limits, restricting the measured mobility values. As time has progressed, graphene preparation techniques have improved, causing measured graphene mobility to approach its intrinsic limits [1-5], which are dictated by the electron-lattice interactions. Here we develop Monte Carlo type methodologies to predict these intrinsically limited graphene mobility values, and their temperature dependence between 200 K and roughly the room temperature.

In this work, we semi-classically calculate transport properties of graphene electrons. Therefore here they are not relativistically described using the Dirac equation. Further, we consider the interaction of electrons with in-plane longitudinal and transverse, and out-of-plane transverse acoustic and optical one-phonon processes. Equilibrium statistics or adiabatic

conditions are employed for phonons. Moreover, graphene is assumed to be infinite in extent, and without impurities and conformal deformities. To obtain temperature dependent graphene electron mobility under these conditions, we then employ Monte Carlo techniques using full band electronic and phononic graphene dispersion curves. Our calculations indicate that around room temperature graphene exhibits strong temperature dependence. Next, we describe the numerical models we use for the electron-phonon interactions along with theoretical predictions. This is followed by our calculated temperature dependency of graphene electron mobility and resistivity results.

II. ELECTRON SCATTERING RATE

A. Electron and Phonon Dispersion Curves

To model electron transport in graphene using Monte Carlo simulations, we need the electronic and phononic dispersion relations for graphene. By applying the tight-binding method to the four nearest distant neighbors, we obtain the band structures of electrons and phonons. This gives the following analytical energy-momentum relation, which is plotted in Fig. 1, for the graphene electrons.

$$E(k_x, k_y) = \gamma \sqrt{1 + 4 \cos\left(\frac{\sqrt{3}}{2} ak_x\right) \cos\left(\frac{a}{2} k_y\right) + 4 \cos^2\left(\frac{a}{2} k_y\right)} \quad (1)$$

Above, k_x and k_y are momenta that correspond to electron movements that are perpendicular to each other, and at the same time are, respectively, parallel or vertical to any two carbon-carbon bonds of the graphene's unit cell in space. Further, a ($= 2.46 \text{ \AA}$) is the graphene's lattice constant, which is the second nearest distance between the carbons in its unit cell. (The first is the carbon-carbon bond length, which is approximately 1.42 \AA .)

Fig. 1 indicates that we have conduction band minima at the six \mathbf{K} points of the Brillouin zone. Therefore, energy-dispersion relations in the vicinity of these points determine the low-field transport and hence mobility. If we write the momentum with respect to a \mathbf{K} point or as the distance from that point, then a linear energy-momentum relation that represents a cone can be used to approximate (1), as shown below. Here the proportionality constant is Planck's constant multiplied by the graphene electron Fermi velocity, which is one three-hundredth of the speed of light.

$$E(k) = \hbar v_F k \quad (2)$$

For the phononic bands of graphene, four-nearest distant tight-binding method does not provide an analytical expression like it does for electrons, mainly due to the use of different force constants in various directions. For a discretized momentum point, we calculate the six energy eigenvalues (two in-plane and out-of-plane modes for acoustic and optical phonons), corresponding to the three degrees of freedom in space, of the dynamical matrix for lattice vibrations, as described in [5]. This provides energy-momentum relations for the three acoustic and optical phonon branches, which we save

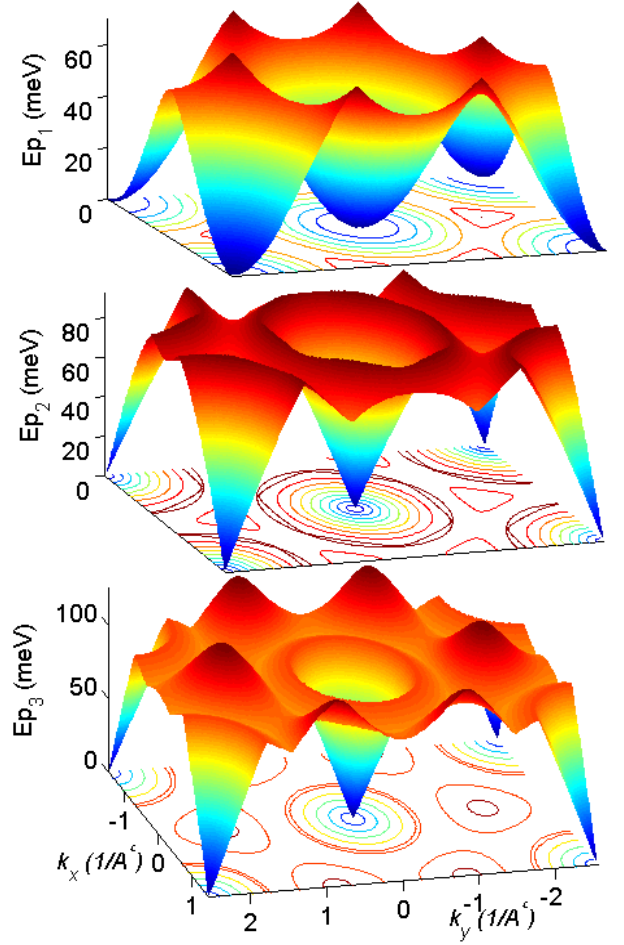


Figure 2. Acoustic phonon branches of graphene calculated using the four nearest neighbor tight-binding method. Ep1 corresponds to the out-of-plane mode while others are for the in-plane modes.

in a look-up table for later use in our Monte Carlo calculations. For example, our calculated acoustic phonon branches are plotted in Fig. 2 using these tables. Here the resolution is approximately 150 points in each momentum direction.

The acoustic branches in the vicinity of Γ points have linear energy-momentum relations like electron dispersion curves near \mathbf{K} points. These acoustic phonons give rise to low energy intravalley scatterings, and are important for low-field transport. Below, we show their dispersion relation (for in-plane modes) as a function of phonon momentum q , which is with respect to the Γ point. It incorporates a proportionality constant that includes the speed of sound in graphene, which is roughly one-hundredth of the graphene electron Fermi velocity.

$$E_p(q) = \hbar v_s q \quad (3)$$

B. Electron-Phonon Scattering Rates

To obtain phonon limited graphene mobility, we first determine graphene scattering rates, as shown in the following, using Fermi's golden rule and the deformation potential approximation. Below, as the energy conservation terms that

are represented by the Dirac-delta functions imply, the first and second terms of the sum account for phonon absorption and emission, respectively. H is the overlap integral for phonon absorption or emission, indicated by a superscript. Further, final or initial momentum $\mathbf{k} = (k_x, k_y)$ includes the effects of both momentum directions.

$$\begin{aligned} \Gamma(\mathbf{k}_i, \mathbf{k}_f) = & \frac{2\pi}{\hbar} |H^a|^2 \delta(E(\mathbf{k}_f) - E(\mathbf{k}_i) - E_p(\mathbf{k}_f - \mathbf{k}_i)) \\ & + \frac{2\pi}{\hbar} |H^e|^2 \delta(E(\mathbf{k}_f) - E(\mathbf{k}_i) + E_p(\mathbf{k}_f - \mathbf{k}_i)) \end{aligned} \quad (4)$$

To obtain overlap integrals in (4) and thus the scattering rate as a function of energy, momentum and other known parameters, we start with the scattering rate formula of lower dimensional carbon nanotubes [7], and change it to a form suitable for the two-dimensional graphene [5]. We then take the integral of (4) within the unit cell in the Brillouin zone to calculate the total scattering rate for an electron with a specific energy and momentum. The resulting total scattering rate, Γ , for a graphene electron with initial momentum \mathbf{k}_i and energy $E(\mathbf{k}_i)$ to all possible final momenta \mathbf{k}_f and energies $E(\mathbf{k}_f)$ such that $E(\mathbf{k}_f) - E(\mathbf{k}_i) \pm E_p(\mathbf{k}_f - \mathbf{k}_i) = 0$, is written below. Here, the electronic and phononic dispersion curves [5] are calculated using the four nearest neighbor tight-binding method, as aforementioned.

$$\begin{aligned} \Gamma(E(\mathbf{k}_i)) = & \frac{\hbar D^2}{4\pi\rho} \int_{\text{BZ}} \frac{Q^2}{E_p(\mathbf{k} - \mathbf{k}_i)} \left[N_p(E_p(\mathbf{k} - \mathbf{k}_i)) + \frac{1}{2} \pm \frac{1}{2} \right] \times \\ & \delta(E(\mathbf{k}) - E(\mathbf{k}_i) \pm E_p(\mathbf{k} - \mathbf{k}_i)) d(\mathbf{k} - \mathbf{k}_i) \end{aligned} \quad (5)$$

Above, D ($=16\text{eV}$) is the graphene deformation potential, ρ is the graphene surface density, Q is a wavevector, $E_p(\mathbf{k})$ is the phononic energy at \mathbf{k} , $N_p(E_p(\mathbf{k}))$ is the Bose-Einstein factor for calculating the phonon occupation number, and other parameters have their usual meanings. Additionally, the integral is taken over the entire Brillouin zone, where $k_x = \left[-\frac{2\pi}{a}, \frac{2\pi}{a} \right] \times \left(\frac{1}{\sqrt{3}} \right)$, $k_y = \left[-\frac{2\pi}{a}, \frac{2\pi}{a} \right]$, $|k_x| + \left| \frac{k_x}{\sqrt{3}} \right| \leq \left(\frac{4\pi}{3a} \right)$ [5], and the lattice constant $a = 2.46\text{\AA}$.

C. Theoretical Electron-Phonon Scattering Rate Temperature Dependence

To theoretically calculate the phonon-limited scattering rate in (5), we make use of the following assumptions (the first two are generally valid around room temperature for most materials):

- Low-energy acoustic phonons determine the low-field electron mobility.
- Phonon energies that are exchanged during emission and absorption are lower than the thermal energy at room temperature, giving rise to the equipartition approximation. This gives the following phonon occupation number as a function of phonon and thermal energies.

$$N_p(E_p(\mathbf{q})) = \frac{E_{\text{th}}}{E_p(\mathbf{q})} \quad (6)$$

- For low phononic energies, phonon dispersion relation can be expressed, as mentioned before for in-plane modes, using a linear energy-momentum relation: $E_p = q\hbar v_s$, where v_s ($\approx 10^6$ cm/s) is the sound velocity in graphene and q is the phonon momentum relative to the nearest Γ point.

- Likewise, for low energies, electron dispersion relation is $E = k\hbar v_F$ where k is the momentum relative to the nearest \mathbf{K} point, v_F ($\approx 10^8$ cm/s) is the Fermi velocity. Therefore, the density of states is $\frac{2\pi}{\hbar v_F} E$ ($= 2\pi k \frac{dk}{dE}$).

Substituting these in (5) and taking Q^2 as $|q|^2$ for acoustic phonons result in the following linear temperature dependency (due to thermal energy E_{th}) for the scattering rate.

$$\Gamma(E(\mathbf{k}_i)) \approx \left(\frac{D^2 E_{\text{th}}}{2\rho\hbar^3 v_s^2 v_F^2} \right) E(\mathbf{k}_i) \quad (7)$$

In the Bloch-Gruneisen transport regime, which is generally at lower temperatures, the above linear relation breaks down, and the scattering rate becomes a strong function of temperature, where $\Gamma \approx T^n$ and $3 < n < 6$. This happens when the phononic energies involved in scatterings are comparable to thermal energies ($q\hbar v_s \geq E_{\text{th}}$; if q is twice the Fermi wavevector for intrinsic graphene then $50\text{K} \geq T$ [9]). Further, due to the conic electronic dispersion curves, electron energies quickly increase due to an applied field. This may necessitate scattering phonons with energies comparable to thermal energies, and thus may give rise to a high temperature dependency. Also, electron scatterings with phonons on graphene samples with conformal deformities might give rise to higher temperature dependencies. Additionally the out-of-plane mode in Fig. 2 has a non-linear energy-momentum relation that may result in a strong temperature dependency [8].

III. MONTE CARLO CALCULATIONS OF TEMPERATURE DEPENDENCE OF MOBILITY /RESISTIVITY

To investigate electron-phonon interactions and electron transport in graphene, we develop a Monte Carlo (MC) simulator that resolves electron transport in conjunction with a semiclassical electron-field interaction, and the phonon-limited scattering rates [5]. This is achieved first by using a high resolution Riemann sum for evaluating the integral in (5) for a given electron energy and momentum. The result of the integral is then used to calculate the total scattering rate (for choosing a correlated drift time or scattering probability) and final likely-to-scatter energy-momentum neighborhoods. In case of a scattering, the final electronic energy and momentum are probabilistically obtained using a Monte Carlo integration technique, while conserving total energy and momentum [5]. Specifically, during the Riemann sum, scattering probabilities

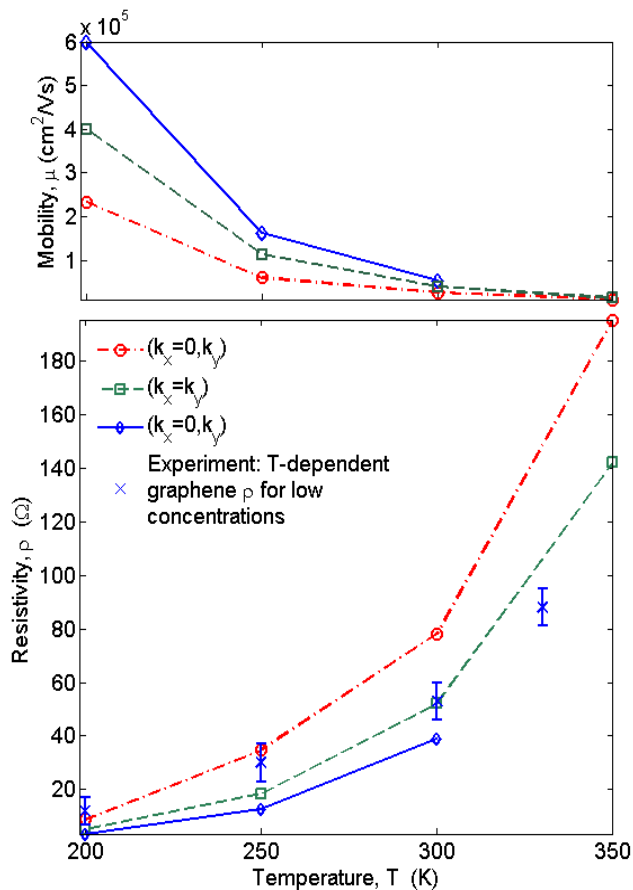


Figure 3. Temperature- and field direction- dependent mobility (top) , and resistivity (bottom) of intrinsic graphene with an intrinsic carrier concentration of $2 \times 10^{12} \text{ cm}^{-2}$. (Field is applied along the graphene k_y direction \circ , $k_x=k_y$ direction \square , and k_x direction \diamond .) We also show experimentally measured temperature-dependent part of graphene resistivity data extracted from the recently published [4] (corresponds to the resistivity of graphene samples with low carrier concentrations — measured at graphene devices' neutrality points) along with error bars in the aforementioned measurements. Experimentally measured resistivity values change as much as the fifth power of temperature. Further, mobility and resistivity curves share the same temperature axis.

to different neighborhoods corresponding to the grids employed for discretization are stored. Then an energy-momentum neighborhood that the electron is likely to scatter is determined stochastically. Since the momentum resolution of this neighborhood is not high enough to resolve low energy transport, and we do not want to be restricted by these discretized values for electron energy and momentum, a Monte Carlo integration technique is employed within this neighborhood to obtain a highly probable energy-momentum point to scatter. Further, in case of no electron-phonon interaction, a total scattering rate correlated drift time is employed for calculating a new momentum and energy for the electron.

Fig. 3 shows our calculated graphene mobility and resistivity values as a function of temperature for three different field directions along with recently measured

temperature dependent graphene resistivity data. In simulations, external fields are applied in directions that give rise to electron accelerations parallel to k_y , $k_x=k_y$, and k_x momentum directions. To calculate resistivity, we use $(en_o\mu)^{-1}$ where e is the electronic charge, n_o is the intrinsic graphene concentration taken as $2 \times 10^{12} \text{ cm}^{-2}$, and μ is our calculated temperature- and field direction-dependent graphene mobility. Fig 3 indicates that phonon-limited low-field intrinsic graphene mobility is very sensitive to temperature changes, T^n where $2 < n < 4$ [4,5,8,10]. We associate this with high energy (relative to thermal energy) phonons that assist electron scatterings, their phonon occupation numbers, the conic shape of the electronic and in-plane phononic dispersion curves, and the non-linear band structure of the out-of-plane phononic branch. In addition, field-direction dependency of graphene mobility is related to the slightly different dispersion curves electrons see in the direction they move.

IV. CONCLUSION

In conclusion, we investigated temperature-dependent graphene electron mobility, and compared our findings to recently published data. They both indicate that temperature-dependent mobility changes, which are related to the electronic and phononic dispersion curves, are unusually high for intrinsic or low doped graphene samples. This may be attributed to the conic band structures, and electron interactions with in- and out-of-plane phonons that have energies comparable to the thermal energy.

REFERENCES

- [1] K. S. Novoselov, A. K. Geim, S. V. Morozov, D. Jiang, Y. Zhang, S. V. Dubonos, I. V. Grigorieva, and A. A. Firsov, "Electric field effect in atomically thin carbon films", *Science*, vol. 306, pp. 666-669, 2004.
- [2] C. Berger, Z. Song, X. Li, X. Wu, N. Brown, C. Naud, D. Mayou, T. Li, J. Hass, A. N. Marchenkov, E. H. Conrad, P. N. First, and W. A. deHeer, "Electronic confinement and coherence in patterned epitaxial graphene", *Science*, vol. 312, pp. 1191-1196, 2006.
- [3] A. K. Geim, and K. S. Novoselov, "The rise of graphene", *Nature Materials*, vol. 6, pp. 183-191, 2007.
- [4] S. V. Morozov, K. S. Novoselov, M. I. Katsnelson, F. Schedin, D. C. Elias, J. A. Jaszczak, and A. K. Geim, "Giant intrinsic carrier mobilities in graphene and its bilayer", *Physical Review Letters*, vol. 100, pp. 016602-1-4, 2008.
- [5] A. Akturk, and N. Goldsman, "Electron transport and full-band electron-phonon interactions in graphene", *Journal of Applied Physics*, vol. 103, pp. 053702-1-8, 2008.
- [6] E. H. Hwang, S. Adam, and S. D. Sarma, "Carrier transport in two-dimensional graphene layers", *Physical Review Letters*, vol. 98, pp. 186806-1-4, 2007.
- [7] A. Akturk, and N. Goldsman, "Self-consistent ensemble monte carlo simulations show terahertz oscillations in single-walled carbon nanotubes", *Journal of Applied Physics*, vol. 102, pp. 073720-1-7, 2007.
- [8] E. Mariani, and F. von Oppen, "Flexural phonons in free-standing graphene", *Physical Review Letters*, vol. 100, pp. 076801-1-4, 2008.
- [9] E. H. Hwang, and S. D. Sarma, "Acoustic phonon scattering limited carrier mobility in 2d extrinsic graphene", *cond-mat arXiv:0711.0754v2*, 2007.
- [10] G. Moos, R. Fasel, and T. Hertel, "Temperature dependence of electron-to-lattice energy transfer in single-wall carbon nanotube bundles", *Journal of Nanoscience and Nanotechnology*, vol. 3(1-2), pp. 145-149, 2003.